Molecular Biology of the Cell
Vol. 21, 2639–2648, August 1, 2010

CFTR-Adenylyl Cyclase I Association Responsible for UTP Activation of CFTR in Well-Differentiated Primary Human Bronchial Cell Cultures

Wan Namkung,* Walter E. Finkbeiner,† and A. S. Verkman*

Departments of *Medicine and Physiology and †Pathology, University of California, San Francisco, CA 94143

Submitted December 7, 2009; Revised June 2, 2010; Accepted June 3, 2010
Monitoring Editor: Benjamin Margolis

Chloride secretion by airway epithelial cells is defective in cystic fibrosis (CF). The conventional paradigm is that CFTR is activated through cAMP and protein kinase A (PKA), whereas the Ca^{2+}-activated chloride channel (CaCC) is activated by Ca^{2+} agonists like UTP. We found that most chloride current elicited by Ca^{2+} agonists in primary cultures of human bronchial epithelial cells is mediated by CFTR by a mechanism involving Ca^{2+} activation of adenylyl cyclase I (AC1) and cAMP/PKA signaling. Use of selective inhibitors showed that Ca^{2+} agonists produced more chloride secretion from CFTR than from CaCC. CFTR-dependent chloride secretion was reduced by PKA inhibition and was absent in CF cell cultures. Ca^{2+} agonists produced cAMP elevation, which was blocked by adenylyl cyclase inhibition. AC1, a Ca^{2+}/calmodulin-stimulated adenylyl cyclase, colocalized with CFTR in the cell apical membrane. RNAi knockdown of AC1 selectively reduced UTP-induced cAMP elevation and chloride secretion. These results, together with correlations between cAMP and chloride current, suggest that compartmentalized AC1–CFTR association is responsible for Ca^{2+}/cAMP cross-talk. We further conclude that CFTR is the principal chloride secretory pathway in non-CF airways for both cAMP and Ca^{2+} agonists, providing a novel mechanism to link CFTR dysfunction to CF lung disease.

INTRODUCTION

Activation of P2Y receptors by extracellular nucleotides such as ATP and UTP plays a crucial role in the regulation of ion transport in airway epithelia by a variety of cellular signaling processes (Bucheimer and Linden, 2004; Okada *et al.*, 2006). In human airways, activation of P2Y receptors increases Cl^- secretion by activating Ca^{2+}-activated chloride channel(s) (CaCC) through the inositol trisphosphate (IP_3)-mediated Ca^{2+}-signaling pathway. Recent studies showed Ca^{2+}-dependent and -independent activation of cystic fibrosis transmembrane conductance regulator (CFTR) by P2Y receptors ($P2Y_2$ and $P2Y_6$) in airway epithelial cells (Stutts *et al.*, 1994; Schreiber and Kunzelmann, 2005; Dulong *et al.*, 2007; Faria *et al.*, 2009; Wong *et al.*, 2009). However, the underlying molecular mechanisms are unknown.

The cAMP/protein kinase A (PKA)–signaling pathway is the major mechanism for activation of CFTR Cl^- channel function in airway epithelial cells, though there is also reported evidence that CFTR can be activated by protein kinase C (PKC) and cGMP-dependent protein kinase (PKG; Picciotto *et al.*, 1992; Berger *et al.*, 1993; Dechecchi *et al.*, 1993; French *et al.*, 1995). cAMP is generated from ATP by adenylyl cyclase (AC). To date, nine G-protein–responsive transmembrane AC (tmAC) isoforms (AC1 to AC9) have been identified and one bicarbonate-regulated soluble AC (sAC). tmAC isoforms are modulated by diverse mechanisms, including heterotrimeric G proteins, protein kinases, and Ca^{2+}/calmodulin. AC1, AC3, and AC8 can be stimulated by Ca^{2+}/calmodulin, though the other tmAC isoforms are insensitive to or inhibited by Ca^{2+} (Hanoune and Defer, 2001; Cooper, 2003; Sadana and Dessauer, 2009). AC1 and AC8 are stimulated directly by Ca^{2+}/calmodulin; AC3 is conditionally stimulated by Ca^{2+}/calmodulin, requiring activation of $G\alpha s$ or forskolin. In intact cells, AC3 is inhibited by increased intracellular Ca^{2+} by activation of Ca^{2+}/calmodulin-dependent protein kinase II (CaMKII; Wayman *et al.*, 1995; Wei *et al.*, 1996); in vitro, the EC_{50} for AC3 activation by free $[Ca^{2+}]$ is greater than that of AC1 or AC8 (Choi *et al.*, 1992; Villacres *et al.*, 1995; Fagan *et al.*, 1996; Masada *et al.*, 2009). AC9 activity is inhibited by Ca^{2+}/calcineurin (protein phosphatase 2B), though a more recent study showed Ca^{2+}-mediated potentiation of AC9 activity via calmodulin and CaMKII (Antoni *et al.*, 1998; Cumbay and Watts, 2005). Ca^{2+} signaling may also regulate PKC-activated cyclases AC2 and AC7 through Ca^{2+}-dependent PKC (Hanoune and Defer, 2001; Cooper, 2003; Sadana and Dessauer, 2009). sAC can be stimulated directly by bicarbonate in synergy with Ca^{2+}, but not by heterotrimeric G protein or forskolin (Jaiswal and Conti, 2003; Litvin *et al.*, 2003).

P2Y receptor activation by purinergic agonists strongly stimulates airway ciliary beat frequency. In human airway epithelia, purinergic stimulation produces a prolonged in-

This article was published online ahead of print in *MBoC in Press* (http://www.molbiolcell.org/cgi/doi/10.1091/mbc.E09–12–1004) on June 16, 2010.

Address correspondence to: Alan S. Verkman (Alan.Verkman@ucsf.edu).

Abbreviations used: AC, adenylyl cyclase; CaCC, Ca^{2+}-activated chloride channel; CaMKII, Ca^{2+}/calmodulin-dependent protein kinase II; CF, cystic fibrosis; CFTR, cystic fibrosis transmembrane conductance regulator; GPCRs, G-protein–coupled receptors; HBE, human bronchial epithelial; PKA, protein kinase A; PKC, protein kinase C; PLC, phospholipase C; sAC, bicarbonate-regulated soluble AC; tmAC, transmembrane AC.

Table 1. PCR primers

Primer name	Accession no.	Forward primer	Reverse primer	Product size (bp)
AC1	NM_021116	GGT GGA TCT GAA CAT GCG TGT G	TAA TGC CCT CCG CTT GTC ATC	448
AC2	NM_020546	CCA CAG AGA ACG GCA AGA TCA G	TGG CTG TGG TGA TGA TCG TGA G	516
AC3	NM_004036	TGG AAT TGG ACT GGT GTT GGA C	TCA TCT TCA CCT CCA GCG ACT G	467
AC4	NM_139247	AGT GGC AGT ACG ACG TTT GGT C	GAG CTG CTC AAT GAC CTG GAA G	497
AC5	NM_183357	CAT CTG GTG GAC CGT GTT CTT C	GAA GCC CTC GAT GTC AGC AAA C	451
AC6	NM_015270	TCC ACC TGC AGC ATG AGA ATC G	CCA CGC GCA TGT TCA CAT TC	435
AC7	NM_001114	AAG CTG GCC ATC ATC GAA C	CAC ACG TCA TAC TGC CAC TTG	449
AC8	NM_001115	CAT TGG CAG CAC CTA CAT GG	TGG GTT GGG TTG GAC TCT TC	429
AC9	NM_001116	TTG CGG TCC ACA TGA GAT CC	GCT TCA TCC CGG AAA TGG TAG	400

crease of ciliary beat frequency via Ca^{2+}-mediated cAMP production involving activation of tmACs (Morse *et al.*, 2001; Lieb *et al.*, 2002; Nlend *et al.*, 2007). In several systems the cAMP-signaling pathway is defined by its precise spatial and temporal regulation in which specific tmACs can selectively regulate closely associated proteins (Willoughby and Cooper, 2007). On the basis of these many observations, we postulated the possibility of CFTR activation by apical membrane localized Ca^{2+}-dependent tmACs in human airway epithelium.

Using well-differentiated primary cell cultures of human airway epithelia, we report here that the majority of Cl^- current in response to Ca^{2+} agonists is carried by CFTR by a mechanism involving compartmentalized, Ca^{2+}-dependent activation of AC isoform AC1. These data establish a novel molecular-level mechanism for CFTR activation in a CF disease-relevant cell type and provide new insight into lung disease pathogenesis in CF.

MATERIALS AND METHODS

Material and Solutions

Amiloride, H-89, uridine 5′-triphosphate (UTP), ionomycin, U73122, GF109203X, Go6983, forskolin, 3-isobutyl-1-methylxanthine (IBMX), 1,2-bis-(*o*-aminophenoxy)-ethane-*N*,*N*,*N*′,*N*′-tetraacetic acid, tetraacetoxymethyl ester (BAPTA/AM), and other chemicals, unless otherwise indicated, were purchased from Sigma-Aldrich (St. Louis, MO). SQ22536, PD153035, phorbol 12-myristate 13-acetate (PMA), 2-[*N*-(2-hydroxyethyl)]-*N*-(4-methoxybenzenesulfonyl)] amino-*N*-(4-chlorocinnamyl)-*N*-methylbenzyl-amine (KN-93), and *N*-(6-aminohexyl)-5-chloro-1-naphthalenesulfonamide (W-7) were purchased from Calbiochem (San Diego, CA). $CFTR_{inh}$-172 and $CaCC_{inh}$-A01 were synthesized as described (Ma *et al.*, 2002; De La Fuente *et al.*, 2008). The HCO_3^--buffered solution contained (in mM): 120 NaCl, 5 KCl, 1 $MgCl_2$, 1 $CaCl_2$, 10 D-glucose, 5 HEPES, and 25 $NaHCO_3$ (pH 7.4). The HEPES-buffered solution contained (in mM): 140 NaCl, 5 KCl, 1 $MgCl_2$, 1 $CaCl_2$, 10 D-glucose, and 10 HEPES (pH 7.4).

Cell Culture

Human bronchial epithelial (HBE) cells (non-CF and CF) were cultured at an air–liquid interface at 37°C in 5% CO_2/95% as described previously (Yamaya *et al.*, 1992). Briefly, cells were dissociated by enzymatic digestion, suspended in a 1:1 mixture of DMEM and Ham's F-12 medium containing 5% fetal calf serum (Hyclone, Logan, UT), gentamicin (50 μg/ml), penicillin (100 U/ml), streptomycin (1 mg/ml), and fungizone (2.5 μg/ml), and seeded at a density of 10^6 cells/cm^2 onto 12-mm diameter Snapwell polycarbonate inserts (0.4-μm pore size; Costar, Corning, NY) overlaid with a thin coat (15 μg/cm^2) of human placental collagen (Sigma-Aldrich). The next day the cells were rinsed with PBS, and the medium was replaced with ALI medium containing gentamicin, penicillin, and streptomycin at the concentrations given above. The medium was changed every 3 d. Transepithelial resistance was measured using an epithelial volt-ohmmeter (World Precision Instruments, Sarasota, FL). Cultures were used 21 d after plating, at which time full mucociliary differentiation was confirmed by histology, resistance range was 500-1200 $\Omega \cdot cm^2$, and a thin airway surface liquid film was seen.

Electrophysiology

HBE cells grown on permeable supports (Snapwell, 1.12-cm^2 surface area) were mounted in Ussing chambers (Physiological Instruments, San Diego, CA). Cells were bathed for a 30-min stabilization period in HCO_3^--buffered solution and aerated with 95% O_2/5% CO_2 at 37°C. Short-circuit current (Isc) was measured using an EVC4000 Multi-Channel V/I Clamp (World Precision Instruments) and recorded using PowerLab/8sp (AD Instruments, Castle Hill, Australia). In some experiments, for measurement of apical Cl^- conductance, the basolateral membrane of HBE cells was permeabilized with nystatin (360 μg/ml), and a Cl^- gradient was applied in which the apical membrane was bathed with the HCO_3^--buffered solution and in the basolateral solution 120 mM NaCl was replaced by Na gluconate. Isc was recorded continuously with agonists/inhibitors added at specified times. The apical epithelial sodium channel (ENaC) was inhibited by 10 μM amiloride. Transepithelial resistance was calculated using Ohm's law from current changes in response to 10-mV pulses.

RT-PCR

Expression of mRNA encoding AC1–9 was determined by RT-PCR in primary cultures of HBE cells. Total RNA was extracted by using a Trizol solution (Invitrogen, Carlsbad, CA) and reverse-transcribed by using random hexamer primers and a ribonuclease H-reverse transcriptase (Invitrogen). The cDNA was amplified with specific primers and Taq polymerase (Invitrogen). Primer sequences are provided in Table 1.

Real-Time RT-PCR

cDNA was prepared from HBE cells as described above. Fluorescence-based quantitative RT-PCR was carried out using the LightCycler 480 instrument with LightCycler FastStart DNA MasterPLUS SYBR Green I kit (Roche Diagnostics, Alameda, CA). The thermal cycling conditions comprised an initial step at 95°C for 5 min followed by 40 cycles at 95°C for 10 s, 60°C for 10 s, and 72°C for 10 s. The amount of AC1 and AC9 mRNA was normalized to that of β-actin by using the $2^{-}\Delta\Delta CT$ (CT, threshold cycle) method (Livak and Schmittgen, 2001), $\Delta\Delta CT = (CT_{ACs} - CT_{\beta\text{-actin}})_{ACs\_siRNA} - (CT_{ACs} - CT_{\beta\text{-actin}})_{control\_siRNA}$. The primer sequences used were as follows: AC1 sense, 5′-AAA TGT TCA AGG CCG AGA TCC-3′; AC1 antisense, 5′-TTT CCG AGG CTG TTC TTA ATG C-3′; size of AC1 PCR product, 87 base pairs; AC9 sense, 5′-TTG CGG TCC ACA TGA GAT CC-3′; AC9 antisense, 5′-CAG AAA GAA GCC CAC ACA CAC-3′; size of AC9 PCR product, 83 base pairs; and β-actin sense, 5′-GCA AAG ACC TGT ACG CCA ACA C-3′; β-actin antisense, 5′-ATC TCC TTC TGC ATC CTG TC-3′; size of β-actin PCR product, 82 base pairs.

Immunocytochemistry

Immunostaining of human airway epithelial monolayers was performed using antibodies against AC1 (sc-586; Santa Cruz Biotechnology, Santa Cruz, CA), AC9 (sc-8576, Santa Cruz Biotechnology), acetylated α-tubulin (T7451, Sigma-Aldrich), and CFTR (M3A7, Upstate Biotechnology, Lake Placid, NY). Briefly, the monolayers were fixed and permeabilized by incubation in cold methanol for 10 min at −20°C. Nonspecific binding was reduced by a 1-h incubation at room temperature with 0.1 ml PBS containing 5% goat serum, 1% bovine serum albumin, and 0.1% gelatin. After blocking, the monolayers were stained with antibodies and then with fluorescent secondary antibody (Invitrogen). Images were collected using a laser-scanning confocal microscope (Nikon, Tokyo, Japan).

Immunoblotting and Immunoprecipitation

Cell lysates from T84 cells and CFTR-transfected human embryonic kidney (HEK)-293 cells were mixed with anti-CFTR antibody and incubated overnight at 4°C in lysis buffer. Immune complexes were collected by binding to

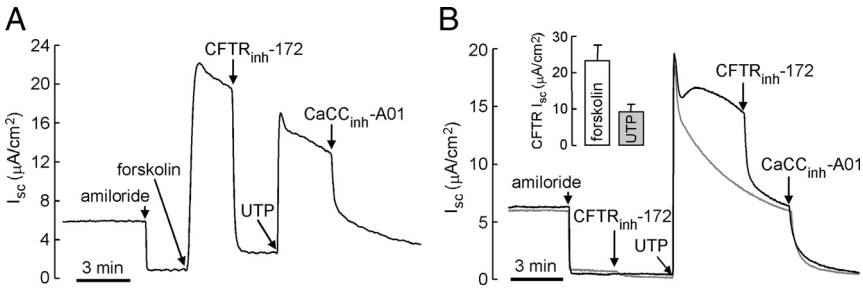

Figure 1. Strong activation of CFTR by UTP in well-differentiated primary cultures of HBE cells. (A) Isc after additions of amiloride (10 μM), forskolin (10 μM), $CFTR_{inh}$-172 (10 μM), UTP (100 μM), and $CaCC_{inh}$-A01 (30 μM), a CaCC-selective inhibitor. (B) Cells were pretreated with $CFTR_{inh}$-172 (10 μM) to block CFTR Cl^- current (gray line). Forskolin and UTP-induced CFTR-dependent Isc (inhibited by $CFTR_{inh}$-172, 10 μM) is summarized in bar graph format (error bars, SE; n = 7).

mixed protein A/G beads and washed four times with lysis buffer before electrophoresis. The lysis buffer contained (in mM): HEPES 50 (pH 7.4), NaCl 150, EDTA 1, Nonidet P-40 1% (vol/vol), glycerol 10% (vol/vol), and the complete protease inhibitor mixture (Roche Applied Science, Indianapolis, IN). The immunoprecipitates and HBE cell lysates were suspended in SDS sample buffer and separated by SDS-PAGE and immunoblotted using standard procedures (transfer to polyvinylidene difluoride membrane, 1-h blocking in 5% nonfat dry milk, primary/secondary antibody incubations, and enhanced chemiluminescence detection).

Small interfering RNA Transfection

siRNAs against AC1 were purchased from Dharmacon (Boulder, CO) as pools of four siRNAs (SMART pools) and from Santa Cruz Biotechnology as pools of three to five siRNAs. siRNA against AC9 was purchased from Dharmacon (SMART pools). siRNA transfection with Lipofectamine 2000 (Invitrogen) was performed according to the manufacturer's protocol. Briefly, HBE cells were washed five times with PBS and small interfering RNA (siRNA; 100 nM) against AC1 or AC9 were transfected with Lipofectamine 2000. Six hours after transfection the solution was replaced with culture medium. The HBE cells were transfected with siRNAs a second time after 24 h incubation. Isc and cellular cAMP were measured 2 d after the second transfection.

Cyclic Nucleotide Assays

HBE cells grown on permeable supports were washed three times with PBS at 37°C and then incubated in PBS at 37°C containing 100 μM IBMX for 5 min in the absence or presence of agonists/inhibitors. After a 5-min incubation, the cells were washed with cold PBS, and cytosolic cAMP was measured using a cAMP immunoassay kit (Parameter cAMP immunoassay kit, R&D Systems, Minneapolis, MN) according to the manufacturer's protocol.

RESULTS

Calcium Agonists Strongly Stimulate CFTR in HBE Cells

Apical membrane chloride conductance was assessed from measurements of Isc in well-differentiated primary cultures of HBE cells. Figure 1A shows evidence for expression of functional cAMP-regulated and Ca^{2+}-regulated chloride channels in these cells, in agreement with prior data (Namkung *et al.*, 2009). After ENaC inhibition by amiloride, the cAMP agonist forskolin produced a robust increase in Isc, which is attributable to CFTR activation as seen by the near-complete inhibition by $CFTR_{inh}$-172. In the continued presence of $CFTR_{inh}$-172 to inhibit CFTR, UTP produced a large increase in Isc that was blocked by the CaCC-selective inhibitor $CaCC_{inh}$-A01. Other calcium-elevating agonists, including ATP, UDP, and ionomycin, produced qualitatively similar responses (data not shown).

Figure 1B provides evidence that the majority of apical membrane chloride current elicited by UTP is carried by CFTR rather than CaCC. In the absence of $CFTR_{inh}$-172 the increase in Isc elicited by UTP was largely blocked by $CFTR_{inh}$-172, with a relatively small effect of $CaCC_{inh}$-A01. Pretreatment with $CFTR_{inh}$-172 before UTP produced a more transient increase in Isc that was inhibited by $CaCC_{inh}$-A01. The figure inset summarizes the CFTR-dependent Isc increase induced by forskolin and UTP, in which $CFTR_{inh}$-172 dependent current at 3–5 min after agonist application was averaged.

Calcium Agonist Stimulation of CFTR Involves AC and PKA Signaling

Further studies were done to support the interpretation of data in Figure 1 that UTP strongly activates CFTR and to determine whether activation involves AC and PKA signaling. Figure 2A shows that pretreatment with the PKA inhibitor H89 largely abolished the activation of CFTR by UTP, as seen by the relatively small inhibition by $CFTR_{inh}$-172. Figure 2B shows that pretreatment with SQ22536, which partially inhibits AC, also reduces CFTR activation by UTP. Figure 2C summarizes the area under the curve for each minute after UTP addition in the presence/absence of $CFTR_{inh}$-172 or H-89. For the first 1 min after UTP addition CaCC-dependent current was ~80% of total current, but later the CaCC and CFTR contributions to current became comparable. Control studies were done in similarly cultured bronchial epithelial cells from cystic fibrosis patients that lack functional CFTR. Figure 2D shows a robust transient UTP response without inhibition by $CFTR_{inh}$-172, which represents a pure CaCC current, and confirms that $CFTR_{inh}$-172 does not inhibit CaCC. UTP-induced current in the CFTR-deficient cells is effectively inhibited by $CaCC_{inh}$-A01. Prior work in CFTR-transfected cells lacking CaCCs verified that $CaCC_{inh}$-A01 at even higher concentrations than used here does not inhibit CFTR (De La Fuente *et al.*, 2008).

Calcium Agonist Stimulation of CFTR Requires Ca^{2+} Elevation

Figure 3A shows similar short-circuit responses after stimulation by UTP or the Ca^{2+} ionophore ionomycin, indicating that Ca^{2+} elevation is sufficient to activate CFTR in the bronchial epithelial cells. Pretreatment with BAPTA to suppress Ca^{2+} elevation produced a marked reduction in the Isc response, indicating that Ca^{2+} elevation is required for CFTR activation (Figure 3B). Figure 3C is a control study showing that BAPTA pretreatment in CFTR-deficient bronchial cells greatly reduces CaCC activation; hence, the BAPTA protocol used here effectively reduces UTP-induced Ca^{2+} elevation. Results from multiple experiments are summarized in Figure 3D. Together, these data support the conclusion that Ca^{2+} elevation is necessary and sufficient for UTP activation of CFTR.

A series of measurements was done to probe other effectors that could be involved in the signaling pathway linking UTP and CFTR activation. Pretreatment with U73122, an inhibitor of phospholipase C (PLC), reduced UTP-induced $CFTR_{inh}$-172–sensitive current by 58 ± 5% (n = 4; Figure 4A). Little or no effect on UTP activation of CFTR was found by treatment of cells with the CaMKII inhibitor KN-93 (Figure 4B), or the epidermal growth factor receptor (EGFR) inhibitor PD153035 (Figure 4C). Bicarbonate-regulated sAC, which produces synergistic activation with $[Ca^{2+}]_i$ is a potential target for GPCR signaling–mediated CFTR activation

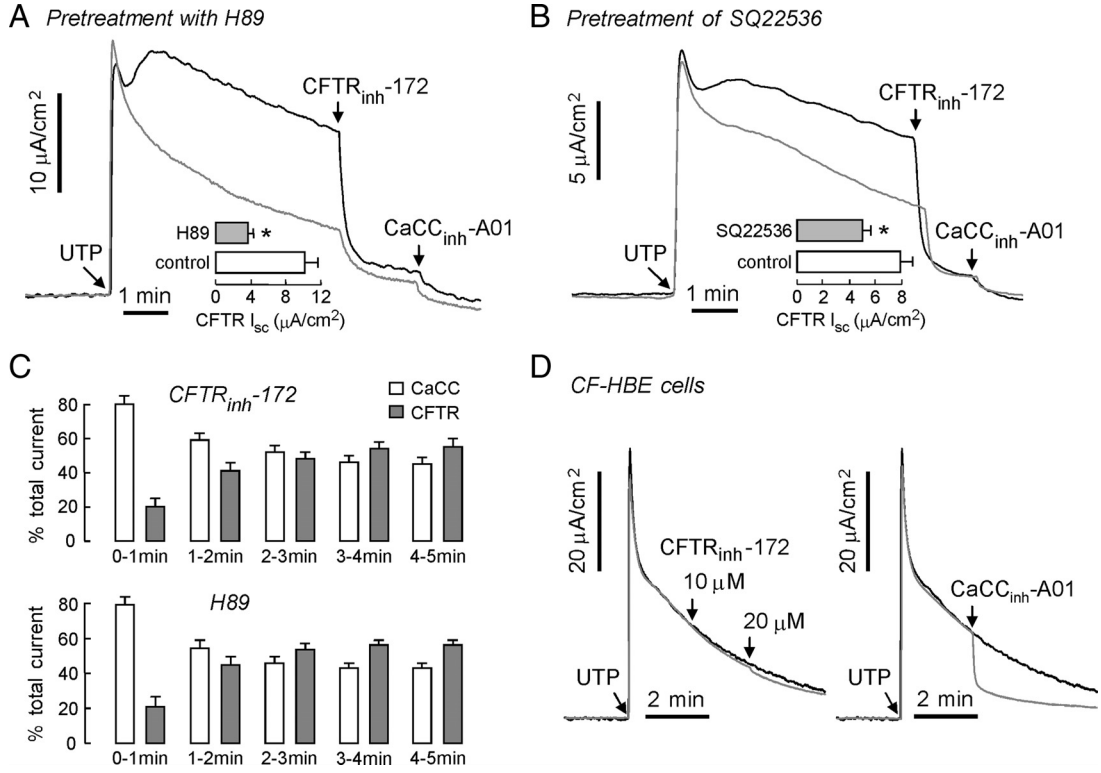

Figure 2. UTP activation of CFTR involves signaling through AC and PKA. Measurements were done in non-CF HBE cells unless otherwise indicated. ENaC activity was blocked by pretreatment of amiloride (10 μM). (A) H-89 (10 μM), a PKA-selective inhibitor, was added to the luminal and basolateral solutions for 30 min before measurement (gray line). UTP-induced CFTR-dependent current was inhibited by $CFTR_{inh}$-172 and remaining CaCC current was blocked by $CaCC_{inh}$-A01. (B) SQ22536 (300 μM), a tmAC-selective inhibitor, was added for 30 min (gray line). UTP-induced CFTR- and CaCC-dependent current was inhibited by $CFTR_{inh}$-172 and $CaCC_{inh}$-A01. (C) CaCC- and CFTR-dependent portion of total current (computed by subtracting $CFTR_{inh}$-172 trace in Figure 1B and the H-89 trace in Figure 2A from the control UTP-induced current trace). (D) $CFTR_{inh}$-172 (left) and $CaCC_{inh}$-A01 (right) effect on UTP-induced current in CF-HBE cells. CFTR-dependent Isc summarized in bar graph format in panels A and B (error bars, SE; n = 4–5). *$p < 0.05$ compared with control.

(Jaiswal and Conti, 2003; Litvin *et al.*, 2003). To determine the effect of sAC on UTP activation of CFTR, UTP-induced CFTR-dependent current was measured in HCO_3^- and HEPES-buffered solution. Ca^{2+} cannot stimulate sAC in the absence of HCO_3^-. Figure 4D shows no significant effect of HCO_3^- on UTP activation of CFTR.

CFTR Activation by UTP Partially Involves PKC Activation

The effect of PKC inhibition on UTP activation of CFTR and PKC-mediated CFTR activation was investigated in the bronchial epithelial cells. Pretreatment with PKC inhibitors, GF109203X and Go6983, reduced UTP-induced $CFTR_{inh}$-172–sensitive current by 19 ± 8 and 8 ± 5%, respectively (n = 4–5; Figure 5, A and B). In contrast, PKA inhibition with H89 blocked UTP-induced $CFTR_{inh}$-172–sensitive current by 63 ± 3% (Figure 2A, n = 5). These results indicate that UTP activation of CFTR is mediated primarily PKA activation and to a much lesser extent by PKC activation.

Apical Membrane CFTR Cl^- Conductance Is Increased by UTP Stimulation

The UTP-induced increase in cytosolic Ca^{2+} could alter the driving force for Cl^- secretion through basolateral Ca^{2+}-activated K^+ channels. To isolate the effect of basolateral Ca^{2+}-activated K^+ channels, we measured apical membrane Cl^- conductance in HBE cells whose basolateral membrane was permeabilized by nystatin and in the presence of an apical-to-basolateral Cl^- gradient. UTP stimulation increased $CFTR_{inh}$-172–sensitive Cl^- current by 9.6 ± 1.2 $\mu A/cm^2$ (n = 5); basal CFTR Cl^- conductance was 2.9 ± 0.7 $\mu A/cm^2$ (Figure 6A). Activation of basolateral Ca^{2+}-activated K^+ channels by 1-ethyl-2-benzimidazolinone (1-EBIO) had minimal effect on basal CFTR activity (Figure 6, B and C). To observe the effect of PKA and ACs on basal CFTR activity, cells were pretreated with H89 or SQ22536, and then $CFTR_{inh}$–172–sensitive current was measured. H89 and SQ22536 had little effect on basal CFTR activity (Figure 6C). These results support the conclusion that UTP activates CFTR in HBE cells.

CFTR Activation Involves Ca^{2+} Agonist–mediated AC1 Activation

The results above suggest that UTP activation of CFTR involves cytoplasmic Ca^{2+} elevation, activation of AC(s), and PKA-mediated CFTR phosphorylation. Of the human AC isoforms, AC1, AC2, AC7, AC8, and AC9 are candidates for transducing the Ca^{2+} signal as they have been reported in some cell types to be activated by Ca^{2+} signaling. RT-PCR analysis of AC isoform expression in the bronchial epithelial cell cultures indicated the expression of transcripts encoding AC isoforms 1, 2, 3, 6, 7, and 9 (Figure 7A). The lack of effect of the PKC inhibitor Go6983 and the PKC activator PMA on cAMP accumulation (Figure 7C) excluded the PKC-activated cyclases AC2 and AC7. Further studies therefore focused in AC1 and AC9. Figure 7B shows apical membrane

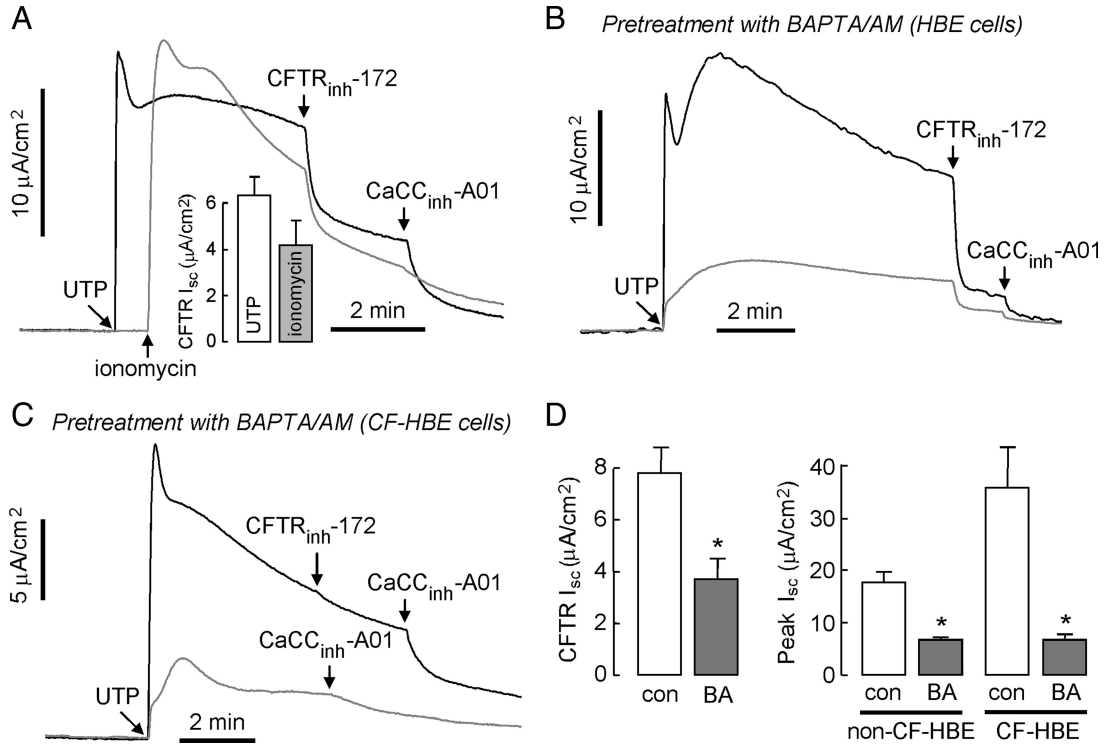

Figure 3. Ca^{2+} elevation is necessary and sufficient for UTP activation of CFTR. Experiments were done in non-CF HBE cells unless otherwise stated. (A) Ionomycin (1 μM, gray line), a Ca^{2+} ionophore, was added to luminal solution, CFTR-dependent current was inhibited by $CFTR_{inh}$-172, and the remaining CaCC current was blocked by $CaCC_{inh}$-A01. CFTR-dependent Isc is summarized in bar graph format (error bars, SE; n = 6). (B) BAPTA-AM (50 μM), a membrane permeable Ca^{2+} chelator, was added to the luminal and basolateral solutions for 30 min before measurements (gray line). CFTR- and CaCC-dependent current were blocked by $CFTR_{inh}$-172 and $CaCC_{inh}$-A01. (C) Effect of pretreatment with BAPTA-AM (gray line) on UTP-induced current in CF-HBE cells. (D) Effect of BAPTA (BA) on CFTR-dependent Isc are summarized in bar graph format (SE; n = 6). UTP-induced peak current in the presence/absence of BAPTA is summarized in the bar graphs (error bars, SE; n = 3–6). *$p < 0.05$ compared with control.

localization of both AC1 and AC9 in the bronchial cell cultures, where CFTR is localized (Puchelle *et al.*, 1992; Kreda *et al.*, 2005). Mosaic staining of AC1 is in agreement with a prior study showing AC1 expression mainly on the apical membrane of ciliated human bronchial cultures (Nlend *et al.*, 2007).

Involvement of AC(s) in the UTP signaling of CFTR activation predicts increased cAMP in response to UTP, provided that the signal is not highly compartmentalized. Figure 7C shows significant elevation of cAMP after UTP or ionomycin. The elevation in cAMP was significantly reduced by inhibition of tmACs and calmodulin by SQ22536

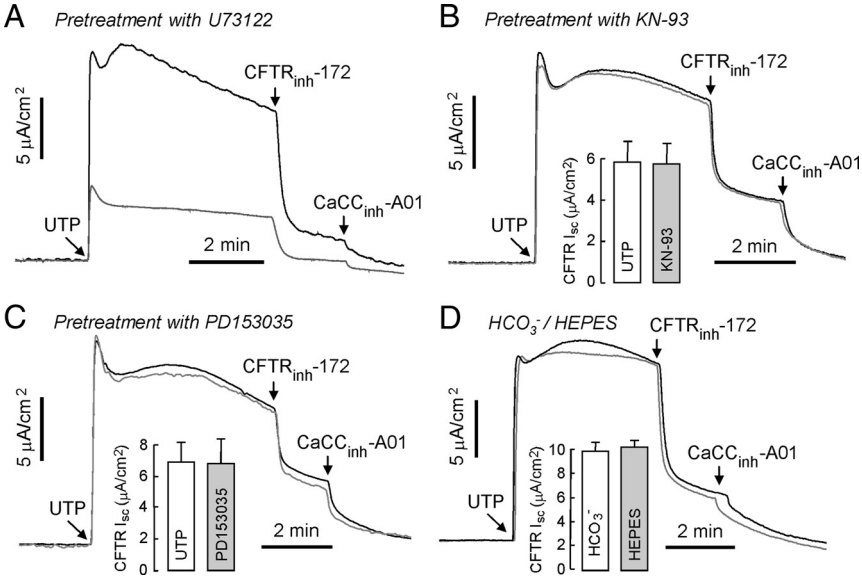

Figure 4. UTP activation of CFTR does not involve CaMKII, EGFR, and sAC. (A) U73122 (10 μM), a PLC inhibitor, was added to the luminal and basolateral solutions for 30 min before measurements (gray line). (B) KN-93 (50 μM), a CaMKII-specific inhibitor, was added to the luminal and basolateral solutions for 30 min before measurements (gray line). (C) PD153035 (1 μM), a selective inhibitor of EGRF tyrosine kinase activity, was added to luminal and basolateral solutions for 30 min (gray line). (D) UTP (100 μM)-induced current was measured in HCO_3^-- and HEPES-buffered solution. CFTR-dependent Isc are summarized in the bar graphs (error bars, SE; n = 3). *$p < 0.05$ compared with control.

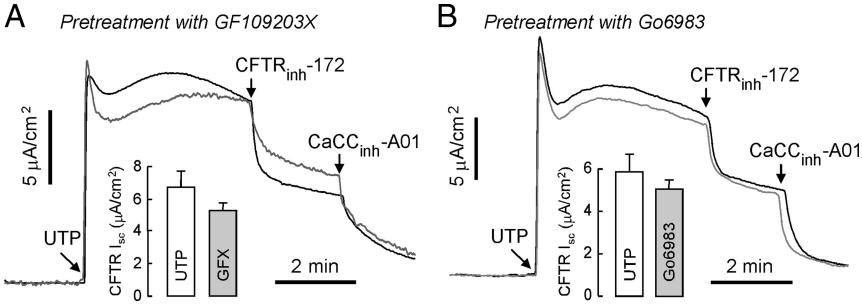

Figure 5. PKC activation is partially involved in UTP activation of CFTR. (A) GF109203X (2 μM), a PKC-specific inhibitor, was added to the luminal and basolateral solutions for 30 min before measurements (gray line). (B) Go6983 (1 μM), a nonselective PKC inhibitor, was added to luminal and basolateral solutions for 30 min before measurements (gray line). CFTR-dependent Isc are summarized in the bar graphs (error bars, SE; n = 3–5).

and W-7, respectively. Notably, the UTP-induced CFTR current was 42% of forskolin-induced maximal CFTR current (Figure 1B); however, the UTP-induced increase in cAMP was >10-fold lower than that induced by forskolin. This observation suggests compartmentalized AC-CFTR signaling.

siRNA knockdown studies were done to investigate whether AC1 and/or AC9 is involved in the Ca^{2+}-induced cAMP response. Figure 8A shows significant reduction in the UTP-induced cAMP accumulation in cells treated with two different AC1 siRNAs but not with AC9 siRNA. Despite considerable work to optimize AC knockdown in the primary bronchial cell cultures, generally only ~50% reduction in AC1 transcript and protein was achieved (Figure 8B). Figure 8C shows partial though significant reduction in the UTP-induced CFTR current with AC1 but not AC9 siRNAs, which was consistent with the cAMP measurements. Together, these results support the conclusion that Ca^{2+} elevation results in cAMP generation by AC1, likely by a compartmentalized signaling mechanism.

Figure 9A shows colocalization of AC1 and CFTR protein, and AC1 and acetylated α-tubulin, a ciliary marker, at the apical membrane of bronchial epithelial cell cultures, consistent with compartmentalized signaling. However, immunoprecipitation studies, done under a variety of conditions, did not indicate direct interaction between AC1 and CFTR protein. Figure 9B shows no AC1 pulldown by CFTR antibody under conditions where EBP50, a known CFTR-interacting protein, was immunoprecipitated. Figure 9C shows a proposed model for UTP-CFTR signaling based on the experimental data, as described further below.

DISCUSSION

Extracellular nucleotides such as ATP and UTP, acting through P2Y receptors, play an important role in human airway epithelia in fluid secretion, cell volume control, ciliary beating, and mucociliary clearance (Lieb *et al.*, 2002; Leipziger, 2003; Lazarowski and Boucher, 2009). Recent studies have demonstrated Ca^{2+}-dependent and -independent activation of CFTR by P2Y receptors in airway epithelial cells (Stutts *et al.*, 1994; Schreiber and Kunzelmann, 2005; Dulong *et al.*, 2007; Faria *et al.*, 2009; Wong *et al.*, 2009). The CFTR-selective inhibitor $CFTR_{inh}$-172 has made it possible to identify CFTR involvement in various cellular responses. We found here that pretreatment with $CFTR_{inh}$-172 remarkably reduced UTP-induced Cl^- secretion in primary cultures of human airway epithelia (Figure 1A). CFTR inhibition by $CFTR_{inh}$-172 and H-89 did not affect the UTP-induced peak current, which was found to be CaCC-dependent, but accelerated the decrease in current (Figure 1B and 2A), indicating that the majority of time-integrated UTP-induced Cl^- current is CFTR-mediated (Figure 2C). Therefore UTP-induced CFTR-dependent current plays a major role in overall Cl^- secretion in HBE cells. CFTR dysfunction in CF therefore produces impairment not only of cAMP induced Cl^- secretion in human airway epithelia, but of Ca^{2+}-induced Cl^- secretion as well.

UTP is a potent agonist of $P2Y_2$ and $P2Y_4$ receptors, which are G-protein–coupled receptors (GPCRs) that are mainly coupled to Gq protein/PLC/IP_3/Ca^{2+} pathways. U73122 inhibition of PLC significantly reduced both UTP-induced initial peak current and $CFTR_{inh}$-172–sensitive current in HBE cells (Figure 4A), suggesting involvement of Gq-cou-

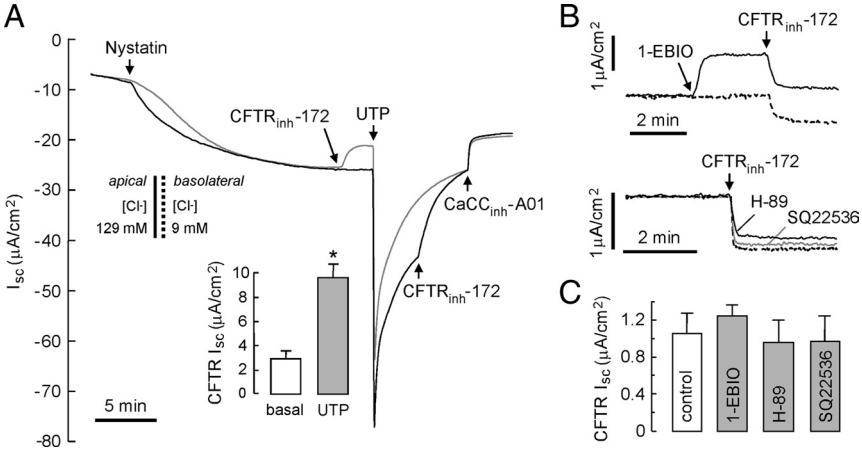

Figure 6. Examination of effects of basolateral Ca^{2+}- activated K^+ channels on UTP activation of CFTR. (A) Apical Cl^- conductance measured after basolateral membrane permeabilization by nystatin (360 μg/ml) and with indicated apical and basolateral solution Cl^-. Cells were pretreated with $CFTR_{inh}$-172 (10 μM) to block basal CFTR Cl^- current (gray line). $CFTR_{inh}$-172 (10 μM), UTP (100 μM), and $CaCC_{inh}$-A01 (30 μM) added as indicated. CFTR-dependent Isc is summarized in bar graph format (SE; n = 4). (B) Effect of activation of basolateral Ca^{2+}-activated K^+ channel and inhibition of PKA and ACs on basal CFTR activity in intact HBE cells. Top, effect of 1-EBIO (1 mM, solid line) on basal CFTR activity (dashed line); bottom, effect of H-89 (10 μM, black line) and SQ22536 (300 μM, gray line) on basal CFTR activity. (C) Effect of 1-EBIO, H-89, and SQ22536 on basal CFTR-dependent Isc are summarized in bar graph format (error bars, SE; n = 4–5). *$p < 0.05$ compared with control.

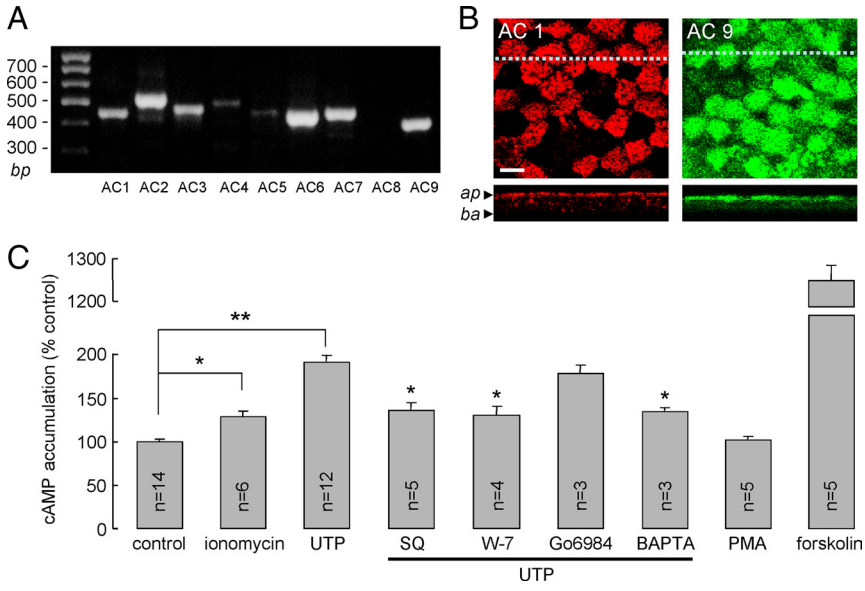

Figure 7. Apical membrane localization of AC1 and AC9 in HBE cells, and UTP-induced cAMP elevation. (A) RT-PCR, using primers specific for AC1–9, was done using as template cDNA from non-CF HBE cells. Gel representative of three sets of amplifications. (B) Immunolocalization of AC1 (red) and AC9 (green) in HBE cells. Top, x-y confocal images just below the cell apical surface, with x-z images shown in the bottom panels. Arrowheads, apical (ap) and basal (ba) membranes. Bar, 10 μm. (C) cAMP accumulation in HBE cells in response to addition of ionomycin (1 μM), UTP (100 μM), PMA (2 μM), and forskolin (10 μM), and pretreatments with SQ22536 (300 μM), W-7 (100 μM), Go6983 (2 μM), and BAPTA-AM (50 μM). Cellular cAMP levels are summarized in bar graph format (error bars, SE). *$p < 0.05$ and **$p < 0.01$.

pled GPCR signaling in UTP-induced CFTR activation. CFTR can be activated by GPCR signaling through activation of PKC and transactivation of EGFR (Yamamoto *et al.*, 2007; van der Merwe *et al.*, 2008). However, we found that inhibition of EGFR by PD153035 did not significantly affect UTP-induced CFTR activation (Figure 4C), and PKC inhibition showed small decreases of $CFTR_{inh}$-172–sensitive current compared with PKA inhibition (Figure 5, A and B, and 2A, respectively). Therefore, UTP-induced CFTR activation is determined mainly by other signaling events downstream of PLC, not including EGFR activation. We therefore focused on P2Y receptor–mediated calcium signaling events.

Intracellular calcium chelation blocked UTP-induced CFTR activation as shown in Figure 3, indicating that intracellular Ca^{2+} elevation is necessary and sufficient for UTP-induced CFTR activation. In human airway epithelia, it has been suggested that purinergic stimulation increases cAMP

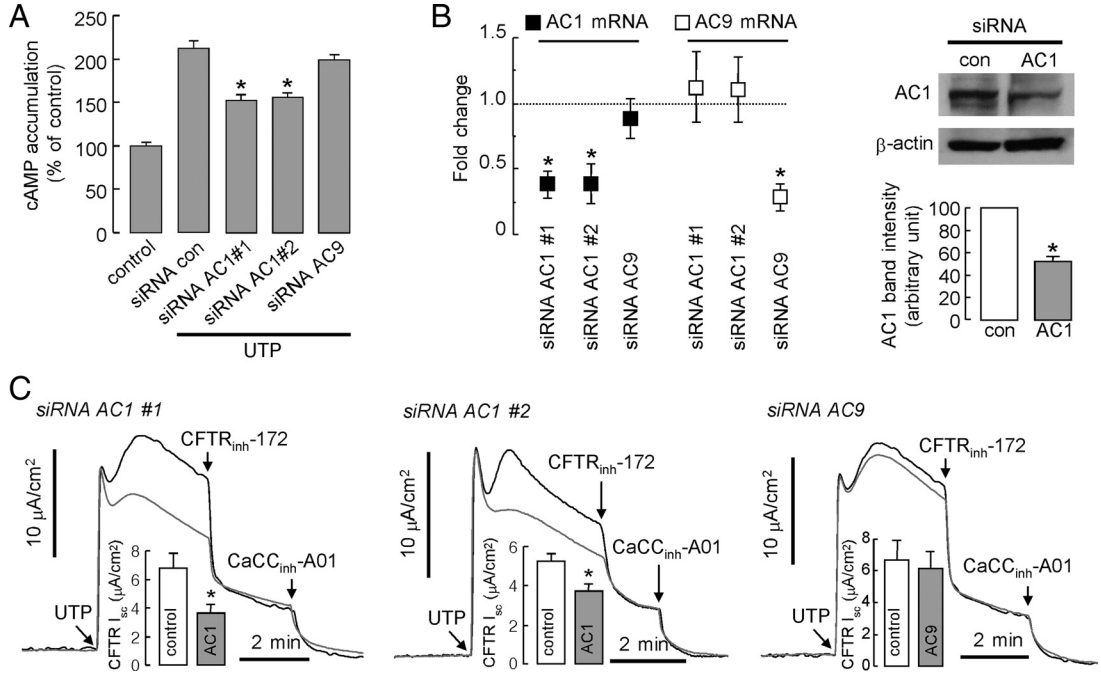

Figure 8. Evidence for AC1 as responsible for cAMP generation after Ca^{2+} elevation. (A) cAMP accumulation in HBE cells measured after transfections with siRNAs (against AC1 and AC9) in response to addition of UTP (100 μM; SE; n = 4–5). (B) Left, relative mRNA expression of AC1 and AC9 as measured real-time RT-PCR; right, AC1 immunoblot at 48 h after transfections with negative control siRNA and siRNA AC1 #1. Band intensities are summarized in bar graph format (error bars, SE; n = 3). (C) AC1 and AC9 were knocked down by siRNAs. UTP-induced activation of CFTR-dependent ($CFTR_{inh}$-172 inhibited) currents measured in siRNAs-treated HBE cells. CFTR-dependent Isc is summarized in bar graph format (error bars, SE; n = 4–5). *$p < 0.05$ compared with control.

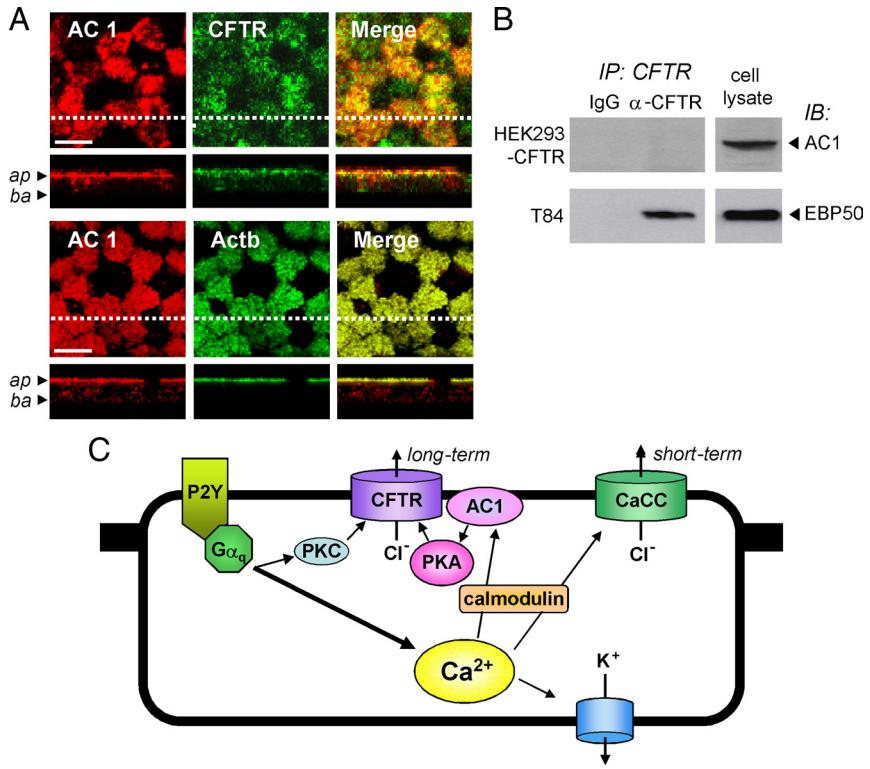

Figure 9. Colocalization of AC1 and CFTR in apical membrane of HBE cells and proposed signaling pathway for CFTR activation after UTP-induced cytoplasmic Ca^{2+} elevation. (A) Immunolocalization of AC1 (red), CFTR (Actb, green), and acetylated α-tubulin (Actb, green) at the apical membrane of HBE cells. Bar, 10 μm. (B) CFTR immunoprecipitation done using cell extracts from HEK-293 cells expressing CFTR and T-84 cells; immunoblot done with antibodies against AC1 and EBP50. Representative of three sets of studies. (C) Proposed mechanism of Ca^{2+}-agonist stimulation of CFTR involving activation of AC1 by a Ca^{2+}/calmodulin-dependent pathway.

production via a Ca^{2+}-mediated pathway (Nlend *et al.*, 2007). We demonstrated cAMP accumulation in the HBE cells after UTP activation of P2Y receptors or ionomycin. Intracellular calcium chelation and inhibition of tmACs and calmodulin by SQ22536 and W-7 significantly blocked UTP-induced cAMP accumulation (Figure 7C). We were unable to study effects of calmodulin inhibition on UTP-induced CFTR activation because the inhibitor W-7 greatly reduced transepithelial resistance (data not shown). Notably, the increase in CFTR current produced by UTP was ~50% of that produced by maximal forskolin (Figure 1B), whereas UTP-induced cAMP accumulation was 10 times less than that induced by forskolin, suggesting compartmentalized tmAC-CFTR signaling.

Greater UTP-induced currents were found previously in CF versus non-CF subjects and primary cultured CF versus non-CF nasal epithelial cells (Knowles *et al.*, 1992); however, in our culture condition, non-CF and CF HBE cells showed similar UTP-induced currents. The average CaCC peak currents were 19.3 ± 1.4 (n = 14) and 23.1 ± 3.7 $\mu A/cm^2$ (n = 10), respectively. This difference may be related to differences in culture condition, individual donor variability, and/or the region (proximal/distal) of airway studied.

Investigation of the role of AC1 and AC9 in UTP-induced CFTR activation in human airway epithelia showed significantly reduced UTP-induced cAMP accumulation and CFTR activation by AC1 but not by AC9 siRNA knockdown (Figure 8). AC1 is stimulated by free Ca^{2+} with an EC_{50} of <0.15 nM in the presence of calmodulin (Choi *et al.*, 1992; Villacres *et al.*, 1995; Masada *et al.*, 2009), consistent with our conclusion that AC1 can be activated by physiological Ca^{2+} elevation. Notably, wild-type CFTR and AC1 have been reported to be expressed predominantly in ciliated cells in human airway epithelia (Puchelle *et al.*, 1992; Kreda *et al.*, 2005; Nlend *et al.*, 2007); our data here show spatial colocalization of AC1 and CFTR protein at the apical membrane of the bronchial epithelial cells, though we were unable by immunoprecipitation to demonstrate direct interaction between AC1 and CFTR. Together, these results support the conclusion that UTP-induced CFTR activation is primarily mediated by activation of AC1 through Ca^{2+} signaling, with compartmentalization of AC1 and CFTR. The concept of compartmentalized signaling involving CFTR has been demonstrated with different receptors and signaling proteins. For example, in Calu-3 cells PKA has been localized with CFTR via ezrin, an AKAP (A-kinase–anchoring protein), and EBP50/NHERF1 (Huang *et al.*, 2000; Sun *et al.*, 2000); compartmentalization of CFTR and PKA is proposed to increase the efficiency of cAMP-mediated Cl^- secretion. Also, the diffusion of newly synthesized cAMP by apical tmACs can be restricted to the apical membrane of airway epithelium by the action of compartmentalized phosphodiesterases (Barnes *et al.*, 2005). Our data here add another molecule, AC1, to the growing list of effectors involved in the complex compartmentalized signaling of CFTR activation.

In summary, we found that UTP-induced CFTR activation is primarily mediated by cAMP signaling through activation of AC1 by Ca^{2+} elevation, indicating major cross-talk between Ca^{2+} and cAMP signaling pathways in HBE cells. Because purinergic stimulation in human airway epithelium inhibits ENaC activity via $P2Y_2$ receptor activation (Boucher, 2007), UTP activation of P2Y receptors regulates each of the major ion channels involved in airway epithelial fluid transport via Ca^{2+} signaling, including CFTR, CaCC, ENaC, and basolateral Ca^{2+}-activated K^+ channel(s). In addition to establishing the molecular details of the signaling pathway for CFTR activation by Ca^{2+} agonists, our findings have important implications for normal airway physiology and airway pathophysiology in CF. In the airways CFTR is expressed in ciliated surface epithelial cells, as

studied here, as well as in serous cells in submucosal glands (Engelhardt *et al.*, 1992; Puchelle *et al.*, 1992; Kreda *et al.*, 2005). Stimulation of substance P receptor, a Gq-coupled GPCR, results in CFTR-dependent elevation of airway gland secretion, which is blocked by Ca^{2+} chelation (Choi *et al.*, 2009). The signaling paradigm established here, of Ca^{2+}-agonist induced CFTR activation, is likely to apply as well to airway submucosal gland epithelia and perhaps to other CFTR-expressing epithelia in the gastrointestinal tract and in exocrine glands.

ACKNOWLEDGMENTS

This work was supported by National Institutes of Health Grants HL73856, DK35124, DK86125, EB00415, EY13574, and DK72517, and Research Development Program and Drug Discovery grants from the Cystic Fibrosis Foundation.

REFERENCES

Antoni, F. A., Palkovits, M., Simpson, J., Smith, S. M., Leitch, A. L., Rosie, R., Fink, G., and Paterson, J. M. (1998). Ca^{2+}/calcineurin-inhibited adenylyl cyclase, highly abundant in forebrain regions, is important for learning and memory. J. Neurosci. *18*, 9650–9661.

Barnes, A. P., Livera, G., Huang, P., Sun, C., O'Neal, W. K., Conti, M., Stutts, M. J., and Milgram, S. L. (2005). Phosphodiesterase 4D forms a cAMP diffusion barrier at the apical membrane of the airway epithelium. J. Biol. Chem. *280*, 7997–8003.

Berger, H. A., Travis, S. M., and Welsh, M. J. (1993). Regulation of the cystic fibrosis transmembrane conductance regulator Cl^- channel by specific protein kinases and protein phosphatases. J. Biol. Chem. *268*, 2037–2047.

Boucher, R. C. (2007). Airway surface dehydration in cystic fibrosis: pathogenesis and therapy. Annu. Rev. Med. *58*, 157–170.

Bucheimer, R. E., and Linden, J. (2004). Purinergic regulation of epithelial transport. J. Physiol. *555*, 311–321.

Choi, E. J., Xia, Z., and Storm, D. R. (1992). Stimulation of the type III olfactory adenylyl cyclase by calcium and calmodulin. Biochemistry *31*, 6492–6498.

Choi, J. Y., Khansaheb, M., Joo, N. S., Krouse, M. E., Robbins, R. C., Weill, D., and Wine, J. J. (2009). Substance P stimulates human airway submucosal gland secretion mainly via a CFTR-dependent process. J. Clin. Invest. *119*, 1189–1200.

Cooper, D. M. (2003). Regulation and organization of adenylyl cyclases and cAMP. Biochem. J. *375*, 517–529.

Cumbay, M. G., and Watts, V. J. (2005). Galphaq potentiation of adenylate cyclase type 9 activity through a Ca^{2+}/calmodulin-dependent pathway. Biochem. Pharmacol. *69*, 1247–1256.

De La Fuente, R., Namkung, W., Mills, A., and Verkman, A. S. (2008). Small-molecule screen identifies inhibitors of a human intestinal calcium-activated chloride channel. Mol. Pharmacol. *73*, 758–768.

Dechecchi, M. C., Tamanini, A., Berton, G., and Cabrini, G. (1993). Protein kinase C activates chloride conductance in C127 cells stably expressing the cystic fibrosis gene. J. Biol. Chem. *268*, 11321–11325.

Dulong, S., Bernard, K., and Ehrenfeld, J. (2007). Enhancement of P2Y6-induced Cl^- secretion by IL-13 and modulation of SK4 channels activity in human bronchial cells. Cell Physiol. Biochem. *20*, 483–494.

Engelhardt, J. F., Yankaskas, J. R., Ernst, S. A., Yang, Y., Marino, C. R., Boucher, R. C., Cohn, J. A., and Wilson, J. M. (1992). Submucosal glands are the predominant site of CFTR expression in the human bronchus. Nat. Genet. *2*, 240–248.

Fagan, K. A., Mahey, R., and Cooper, D. M. (1996). Functional co-localization of transfected Ca^{2+}-stimulable adenylyl cyclases with capacitative Ca^{2+} entry sites. J. Biol. Chem. *271*, 12438–12444.

Faria, D., Schreiber, R., and Kunzelmann, K. (2009). CFTR is activated through stimulation of purinergic P2Y2 receptors. Pfluegers Arch. *457*, 1373–1380.

French, P. J., Bijman, J., Edixhoven, M., Vaandrager, A. B., Scholte, B. J., Lohmann, S. M., Nairn, A. C., and de Jonge, H. R. (1995). Isotype-specific activation of cystic fibrosis transmembrane conductance regulator-chloride channels by cGMP-dependent protein kinase II. J. Biol. Chem. *270*, 26626–26631.

Hanoune, J., and Defer, N. (2001). Regulation and role of adenylyl cyclase isoforms. Annu. Rev. Pharmacol. Toxicol. *41*, 145–174.

Huang, P., Trotter, K., Boucher, R. C., Milgram, S. L., and Stutts, M. J. (2000). PKA holoenzyme is functionally coupled to CFTR by AKAPs. Am. J. Physiol. Cell Physiol. *278*, C417–C422.

Jaiswal, B. S., and Conti, M. (2003). Calcium regulation of the soluble adenylyl cyclase expressed in mammalian spermatozoa. Proc. Natl. Acad. Sci. USA *100*, 10676–10681.

Knowles, M. R., Clarke, L. L., and Boucher, R. C. (1992). Extracellular ATP and UTP induce chloride secretion in nasal epithelia of cystic fibrosis patients and normal subjects in vivo. Chest *101*, 60S–63S.

Kreda, S. M., Mall, M., Mengos, A., Rochelle, L., Yankaskas, J., Riordan, J. R., and Boucher, R. C. (2005). Characterization of wild-type and deltaF508 cystic fibrosis transmembrane regulator in human respiratory epithelia. Mol. Biol. Cell *16*, 2154–2167.

Lazarowski, E. R., and Boucher, R. C. (2009). Purinergic receptors in airway epithelia. Curr. Opin. Pharmacol. *9*, 262–267.

Leipziger, J. (2003). Control of epithelial transport via luminal P2 receptors. Am. J. Physiol. Renal Physiol. *284*, F419–F432.

Lieb, T., Frei, C. W., Frohock, J. I., Bookman, R. J., and Salathe, M. (2002). Prolonged increase in ciliary beat frequency after short-term purinergic stimulation in human airway epithelial cells. J. Physiol. *538*, 633–646.

Litvin, T. N., Kamenetsky, M., Zarifyan, A., Buck, J., and Levin, L. R. (2003). Kinetic properties of "soluble" adenylyl cyclase. Synergism between calcium and bicarbonate. J. Biol. Chem. *278*, 15922–15926.

Livak, K. J., and Schmittgen, T. D. (2001). Analysis of relative gene expression data using real-time quantitative PCR and the $2^{-\Delta\Delta CT}$ method. Methods *25*, 402–408.

Ma, T., Thiagarajah, J. R., Yang, H., Sonawane, N. D., Folli, C., Galietta, L. J., and Verkman, A. S. (2002). Thiazolidinone CFTR inhibitor identified by high-throughput screening blocks cholera toxin-induced intestinal fluid secretion. J. Clin. Invest. *110*, 1651–1658.

Masada, N., Ciruela, A., Macdougall, D. A., and Cooper, D. M. (2009). Distinct mechanisms of regulation by Ca^{2+}/calmodulin of type 1 and 8 adenylyl cyclases support their different physiological roles. J. Biol. Chem. *284*, 4451–4463.

Morse, D. M., Smullen, J. L., and Davis, C. W. (2001). Differential effects of UTP, ATP, and adenosine on ciliary activity of human nasal epithelial cells. Am. J. Physiol. Cell Physiol. *280*, C1485–C1497.

Namkung, W., Song, Y., Mills, A. D., Padmawar, P., Finkbeiner, W. E., and Verkman, A. S. (2009). In situ measurement of airway surface liquid $[K^+]$ using a ratioable K^+-sensitive fluorescent dye. J. Biol. Chem. *284*, 15916–15926.

Nlend, M. C., Schmid, A., Sutto, Z., Ransford, G. A., Conner, G. E., Fregien, N., and Salathe, M. (2007). Calcium-mediated, purinergic stimulation and polarized localization of calcium-sensitive adenylyl cyclase isoforms in human airway epithelia. FEBS Lett. *581*, 3241–3246.

Okada, S. F., Nicholas, R. A., Kreda, S. M., Lazarowski, E. R., and Boucher, R. C. (2006). Physiological regulation of ATP release at the apical surface of human airway epithelia. J. Biol. Chem. *281*, 22992–23002.

Picciotto, M. R., Cohn, J. A., Bertuzzi, G., Greengard, P., and Nairn, A. C. (1992). Phosphorylation of the cystic fibrosis transmembrane conductance regulator. J. Biol. Chem. *267*, 12742–12752.

Puchelle, E., Gaillard, D., Ploton, D., Hinnrasky, J., Fuchey, C., Boutterin, M. C., Jacquot, J., Dreyer, D., Pavirani, A., and Dalemans, W. (1992). Differential localization of the cystic fibrosis transmembrane conductance regulator in normal and cystic fibrosis airway epithelium. Am. J. Respir. Cell Mol. Biol. *7*, 485–491.

Sadana, R., and Dessauer, C. W. (2009). Physiological roles for G protein-regulated adenylyl cyclase isoforms: insights from knockout and overexpression studies. Neurosignals *17*, 5–22.

Schreiber, R., and Kunzelmann, K. (2005). Purinergic P2Y6 receptors induce Ca^{2+} and CFTR dependent Cl^- secretion in mouse trachea. Cell Physiol. Biochem. *16*, 99–108.

Stutts, M. J., Fitz, J. G., Paradiso, A. M., and Boucher, R. C. (1994). Multiple modes of regulation of airway epithelial chloride secretion by extracellular ATP. Am. J. Physiol. *267*, C1442–C1451.

Sun, F., Hug, M. J., Bradbury, N. A., and Frizzell, R. A. (2000). Protein kinase A associates with cystic fibrosis transmembrane conductance regulator via an interaction with ezrin. J. Biol. Chem. *275*, 14360–14366.

van der Merwe, J. Q., Hollenberg, M. D., and MacNaughton, W. K. (2008). EGF receptor transactivation and MAP kinase mediate proteinase-activated receptor-2-induced chloride secretion in intestinal epithelial cells. Am. J. Physiol. Gastrointest. Liver Physiol. *294*, G441–G451.

Villacres, E. C., Wu, Z., Hua, W., Nielsen, M. D., Watters, J. J., Yan, C., Beavo, J., and Storm, D. R. (1995). Developmentally expressed Ca^{2+}-sensitive adeny-

lyl cyclase activity is disrupted in the brains of type I adenylyl cyclase mutant mice. J. Biol. Chem. *270*, 14352–14357.

Wayman, G. A., Impey, S., and Storm, D. R. (1995). Ca^{2+} inhibition of type III adenylyl cyclase in vivo. J. Biol. Chem. *270*, 21480–21486.

Wei, J., Wayman, G., and Storm, D. R. (1996). Phosphorylation and inhibition of type III adenylyl cyclase by calmodulin-dependent protein kinase II in vivo. J. Biol. Chem. *271*, 24231–24235.

Willoughby, D., and Cooper, D. M. (2007). Organization and Ca^{2+} regulation of adenylyl cyclases in cAMP microdomains. Physiol. Rev. *87*, 965–1010.

Wong, A. M., Chow, A. W., Au, S. C., Wong, C. C., and Ko, W. H. (2009). Apical versus basolateral P2Y(6) receptor-mediated Cl^- secretion in immortalized bronchial epithelia. Am. J. Respir. Cell Mol. Biol. *40*, 733–745.

Yamamoto, S., Ichishima, K., and Ehara, T. (2007). Regulation of extracellular UTP-activated Cl^- current by P2Y-PLC-PKC signaling and ATP hydrolysis in mouse ventricular myocytes. J. Physiol. Sci. *57*, 85–94.

Yamaya, M., Finkbeiner, W. E., Chun, S. Y., and Widdicombe, J. H. (1992). Differentiated structure and function of cultures from human tracheal epithelium. Am. J. Physiol. *262*, L713–L724.